

# Zebrafish pancreatic $\beta$ cell clusters undergo stepwise regeneration using Neurod1-expressing cells from different cell lineages

Hiroki Matsuda (✉ [hmatsud1@fc.ritsumei.ac.jp](mailto:hmatsud1@fc.ritsumei.ac.jp))

College of Life Sciences, Ritsumeikan University <https://orcid.org/0000-0001-8639-2719>

Yukihiko Kubota

College of Life Sciences, Ritsumeikan University,

---

## Article

## Keywords:

**Posted Date:** February 3rd, 2022

**DOI:** <https://doi.org/10.21203/rs.3.rs-1311427/v1>

**License:**   This work is licensed under a Creative Commons Attribution 4.0 International License.

[Read Full License](#)

---

# Abstract

Pancreatic  $\beta$  cell clusters produce insulin and play a central role in glucose homeostasis. The regenerative capacity of mammalian  $\beta$  cells is limited and the loss of  $\beta$  cells causes diabetes. In contrast, zebrafish  $\beta$  cell clusters have a high regenerative capacity, making them an attractive model to study  $\beta$  cell cluster regeneration. How zebrafish  $\beta$  cell clusters regenerate, when the regeneration process is complete, and the identification of the cellular source of regeneration are fundamental questions that require investigation. Here we demonstrate that pancreatic  $\beta$  cell cluster regeneration is completed within 13 days after  $\beta$  cell ablation via a two-step regeneration process, that is regenerating function, and then morphology. Additionally, we found that all regenerating pancreatic  $\beta$  cells arose from Neurod1-expressing cells and that cells from different lineages contribute to both functional and morphological regeneration. Together, these results shed light on the fundamental cellular mechanisms underlying  $\beta$  cell cluster regeneration.

## Introduction

Pancreatic  $\beta$  cells are essential for glucose homeostasis as they secrete insulin, the only hormone capable of lowering blood glucose levels. To function normally, vertebrate  $\beta$  cells form a cluster in the pancreatic islet. However, mammalian  $\beta$  cell clusters are poorly regenerative and loss of  $\beta$  cells leads to a reduction of insulin secretion, followed by the development of diabetes. In contrast to mammals, the teleost zebrafish can regenerate  $\beta$  cell clusters throughout their life<sup>1 2 3 4</sup>. Therefore, understanding how and why this fish can regenerate its  $\beta$  cell clusters could provide unique information for mammalian regeneration of these cells.

It has been reported in larval zebrafish that new  $\beta$  cells appear 2 days post- $\beta$  cell ablation (dpa)<sup>1,2</sup>. It is not clear how the  $\beta$  cell numbers recover and when the cluster regeneration is complete. It has also been suggested that  $\alpha$  cells contribute to this regeneration through transdifferentiation<sup>5</sup>; however, at most, their contribution has been reported to be 13%<sup>5</sup>. Furthermore, there are also reports that centroacinar cells and ductal progenitor cells, which contribute to islet neogenesis, and other endocrine progenitor cells also contribute to  $\beta$  cell regeneration<sup>6 7 8</sup> although it is unclear how much these cell types contribute to  $\beta$  cell cluster regeneration. Thus, the process of  $\beta$  cell cluster regeneration in zebrafish currently has various fundamental questions which require investigation, including which cells are the main sources of the regenerating  $\beta$  cells.

In this study, we decided to investigate the regeneration phenomenon in detail, focusing on determining (1) how  $\beta$  cell clusters regenerate, (2) when the process of  $\beta$  cell cluster regeneration is complete, and (3) which cells are the main source of regeneration for  $\beta$  cells. Several transgenic lines that are useful for analyzing cell differentiation and cell lineages were used. Our results showed that the number of  $\beta$  cells increased until 3 dpa, temporarily stopped increasing, then started increasing again after recovering  $\beta$  cell cluster functionality, and finally recovered to the normal number by 13 dpa. On the other hand, whole glucose levels were recovered by 5 dpa. This suggests that zebrafish  $\beta$  cell clusters regenerate

functionality and morphology in a stepwise manner. In addition, we found that all regenerating  $\beta$  cells arise from Neurod1-expressing cells, suggesting that Neurod1-expressing cells are the main source of regeneration. Furthermore, our results suggest that  $\beta$  cells in the phase of “functional regeneration” arose from Neurod1-expressing cells, which already existed in the islets, and that the Neurod1-expressing cells in the “morphological regeneration” phase were newly generated after functional regeneration. These results shed light on the fundamental cellular mechanisms underlying  $\beta$  cell cluster regeneration.

## Results

### Changes in $\beta$ cell number and whole glucose levels during $\beta$ cell cluster regeneration

To understand how and to what point the regeneration of  $\beta$  cell clusters proceeds, we observed the changes in the morphology of pancreatic islets and the cell number of  $\beta$  cell clusters after  $\beta$  cell ablation. In this study,  $\beta$  cell ablation was performed using the nitroreductase/metronidazole (NTR/Mtz) method<sup>1 2</sup>. First, we ablated  $\beta$  cells from *ins:Switch/gcga:GFP/ins:NTR* lines via treatment with 24 h of Mtz between 3 and 4 days post-fertilization (dpf), and then observed the morphological changes of  $\beta$  cell clusters until 15 dpa (19 dpf) (Fig. 1A). We found that the first  $\beta$  cells appeared by 2 dpa and almost the same size and morphology as the  $\beta$  cell clusters of controls were regenerated by 15 dpa, (Fig. 1A). Next, we monitored changes in cell number in the  $\beta$  cell clusters using *ins:H2BGFP/ins:NTR* transgenic lines. Zebrafish have two types of islets, a principal islet, which is a single, huge islet, and secondary islets, which are multiple smaller islets (Fig. 1B and C). The principal islet develops during embryogenesis, followed by multiple secondary islets during postembryonic development<sup>9 10</sup>. When we first counted the  $\beta$  cell number in the principal islet, we found the first  $\beta$  cells on 2 dpa (6 dpf). Although the  $\beta$  cell number increased until 3 dpa (7 dpf), the increase temporarily paused at 7 dpa (11 dpf). After 7 dpa,  $\beta$  cells started increasing again. Finally, the number recovered to the same level as that of the developing principal islet by 13 dpa (17 dpf) (Fig. 1D). When we next counted the  $\beta$  cell number in the secondary islet, we found no clear difference in the  $\beta$  cell number between the developing and regenerating pancreas during our period of observation (Fig. 1E). On the other hand, we found that the total number of  $\beta$  cells in the pancreas (sum of the number of  $\beta$  cells in the principal and secondary islets) showed the same pattern as that in the principal islet (Fig. 1D). Together, our results indicate that zebrafish  $\beta$  cell clusters can recover cell numbers to a normal level by 13 dpa. In addition, under our experimental conditions, we did not find that  $\beta$  cell ablation affected secondary islet development. Therefore, in the remainder of our experiments, we analyzed phenotypes in only the principal islet, but not secondary islets, after  $\beta$  cell ablation.

It has previously been reported that whole glucose levels recovered within several days after  $\beta$  cell regeneration<sup>5</sup>. To confirm these results and to estimate when  $\beta$  cell cluster function was recovered, we next monitored whole glucose levels in *ins:H2BGFP/ins:NTR* lines treated with or without Mtz, from 3 to 17 dpf (Fig. 1G). We found that whole glucose levels became high immediately after  $\beta$  cell ablation. However, whole glucose levels peaked at 2 dpa (6 dpf), followed by recovery by 5 dpa (9 dpf) (Fig. 1G). These results imply that the functionality of the  $\beta$  cell clusters was recovered by 5 dpa. Interestingly, there

is a gap in the recovery timing between glucose levels and cell number after  $\beta$  cell ablation (Fig. 1D, F, and G). This may suggest that  $\beta$  cell clusters undergo a two-step regeneration process, first regenerating functionality in a morphologically incomplete state by 5 dpa and then regenerating morphology by 13 dpa.

### Regenerating $\beta$ cells arise from cells in contact with $\alpha$ cells

It has previously been reported that some  $\beta$  cells arise from  $\alpha$  cells (*gcca*:GFP positive glucagon-expressing cells) after  $\beta$  cell ablation, albeit at a low frequency<sup>5 11</sup>. To confirm the relationship between regenerating  $\beta$  cells and  $\alpha$  cells, we decided to investigate changes in  $\alpha$  cell numbers after  $\beta$  cell ablation. As a result, the number of  $\alpha$  cells itself was not significantly different from that of the control, although the size of the islet became somewhat smaller after  $\beta$  cell ablation (Fig. 2A and B). Using the *gcca*:GFP/*ins*:Switch/*ins*:NTR line, we next examined the correlation between regenerating  $\beta$  cells and  $\alpha$  cells after  $\beta$  cell ablation. These results demonstrated that approximately 15% of *ins*:Switch-expressing regenerating  $\beta$  cells were *gcca*:GFP-expressing cells (Fig. 2C), but that the remaining 85% of the *ins*:Switch-expressing cells were adjacent to *gcca*:GFP-expressing cells (Fig. 2D). Interestingly, *ins*:Switch-expressing cells with *gcca*:GFP-expression were always adjacent to other *gcca*:GFP-expressing cells (Fig. 2C). These results indicated that all regenerating  $\beta$  cells arise from cells adjacent to  $\alpha$  cells.

### All regenerating $\beta$ cells arise from Neurod1-expressing cells

Neurod1, which plays an important role in islet development, is known as a pan-endocrine marker<sup>10 12 13, 14</sup>. To investigate the relationship between Neurod1-expressing cells and regenerating  $\beta$  cells, we examined changes in *neurod1*:EGFP expression and *ins*:Switch expression using *neurod1*:EGFP/*ins*:Switch/*ins*:NTR lines after  $\beta$  cell ablation. *ins*:Switch expression was always observed in *neurod1*:eGFP-expressing cells at both 2 and 3 dpa (6 and 7 dpf; Fig. 3A and B). These results suggest, as one possibility, that Neurod1-expressing cells are the main source of regenerating  $\beta$  cells. Therefore, we next generated *neurod1*:Cre transgenic lines and performed cell lineage-tracing experiments using the *neurod1*:Cre/*ins*:Switch/*ins*:NTR triple transgenic line. In the *neurod1*:Cre/*ins*:Switch (*Tg(insulin:loxP:mCherrySTOP:loxP:H2B-GFP;cryaa:Cerulean*)) line,  $\beta$  cells that arose from non-Neurod1-expressing cells expressed only mCherry, while  $\beta$  cells that arose from Neurod1-expressing cells expressed H2BGFP. These phenotypic analyses showed that all regenerating  $\beta$  cells expressed H2BGFP in a loxp-dependent manner at 13 dpa (17 dpf; Fig. 3C). These results support the possibility that regenerating  $\beta$  cells always arise from Neurod1-expressing cells (N1 cells).

### The cell lineage of N1 cells that contribute to early and late regeneration is different

There have already been abundant N1 cells in the principal islet just prior to and after  $\beta$  cell ablation. To know if the number of N1 cells sufficient for  $\beta$  cell cluster regeneration already existed in the islets just after  $\beta$  cell ablation, we next generated a *neurod1*:CreERT2 transgenic line, and established *neurod1*:CreERT2/*ins*:Switch/*ins*:NTR lines for lineage tracing experiments. For these experiments, *neurod1*:CreERT2/*ins*:Switch/*ins*:NTR lines were treated with or without Mtz from 3 to 4 dpf and with 4-

*Hydroxy Tamoxifen* (4OHT) from 4 to 5 dpf, and then their phenotypes were analyzed (Fig. 4A). We first observed phenotypes of developing  $\beta$  cells in *neurod1:CreERT2/ins:Switch/ins:NTR* lines without Mtz. We found that most of the  $\beta$  cells in the principal islet expressed H2BGFP at both 9 and 17 dpf, although faint mCherry signals remained in some H2BGFP-positive cells (Fig. 4B and C). In contrast, in secondary islets,  $\beta$  cells expressed mCherry, but not H2BGFP (Fig. 4 C). These results indicated that N1 cells, which are necessary for  $\beta$  cell development in the principal islet, are already present in the pancreas by 5 dpf, but that N1 cells, which are the source of  $\beta$  cell development in secondary islets, develop after 5 dpf. Next, we analyzed phenotypes of these transgenic lines after  $\beta$  cell ablation. After  $\beta$  cell ablation, all regenerating  $\beta$  cells expressed H2BGFP at 5 dpa in the principal islet, although mCherry signals remained in some cells (Fig. 4E and H). However, single mCherry-expressing cells appeared by 7 dpa in the pancreas of some zebrafish. The number of single mCherry-expressing cells increased after 9 dpa (Fig. 4F–H). On the other hand, the number of H2BGFP-expressing cells did not change between 5 and 13 dpa (Fig. 4E–H). In addition, the total number of H2BGFP- and single mCherry-expressing cells was shown to have a similar pattern to the results of Fig. 1D (Fig. 4H). These results suggest that all regenerating  $\beta$  cells are generated from N1 cells by 5 dpa (9 dpf), which are already present in the principal islet by 1 dpa (5 dpf), and that N1 cells, which are the source of  $\beta$  cells after 5 dpa, are newly generated after 1 dpa.

### **Most new Neurod1-expressing cells generate after 7 dpa**

To investigate when new N1 cells, which become the source of  $\beta$  cells after 5 dpa, are generated we treated *neurod1:CreERT2/ins:Switch/ins:NTR* lines again with 4OHT at a time point between 4 and 11 dpa after treatment with Mtz and 4OHT, as previously investigated, and then analyzed mCherry and H2BGFP expression at 17 dpf (Fig. 5A). In these transgenic lines treated with a second treatment of 4OHT at 4 to 5 or 6 to 7 dpa, the number of H2BGFP-expressing cells and the area of mCherry-expressing cells did not significantly change compared to controls which did not receive a second 4OHT treatment (Fig. 5B, C, F, and G). However, in transgenic lines treated with a second 4OHT treatment at 8 to 9 or 10 to 11 dpa, the number of H2BGFP-expressing cells increased and the area of mCherry-expressing cells was reduced significantly (Fig. 5D, E, F, and G). These results suggest that most of the new N1 cells for regenerating the morphology of  $\beta$  cell clusters are produced after 7 dpa.

## **Discussion**

In this study, we analyzed the  $\beta$  cell cluster regeneration process using several larval zebrafish transgenic lines to understand which cells were utilized during  $\beta$  cell cluster regeneration and how zebrafish  $\beta$  cell clusters are regenerated. Our results showed that newly formed  $\beta$  cells appeared by 2 dpa and that the number of  $\beta$  cells increased until 3 dpa at which time they stopped increasing. On the other hand, whole glucose levels increased immediately after  $\beta$  cell ablation, peaked at 2 dpa, then decreased and recovered to normal levels by 5 dpa. Thus, the timing of the decrease of whole glucose levels coincided with that of the increase in  $\beta$  cell number. This suggests that the reduction of whole glucose levels after 2 dpa was due to the regeneration of functional  $\beta$  cells in the islets. Interestingly, after whole glucose levels became normal,  $\beta$  cell numbers increased again and eventually recovered to normal levels by 13 dpf. These

findings suggest that zebrafish  $\beta$  cell clusters undergo a two-step regeneration process: first, their  $\beta$  cell clusters regenerate functionally under the conditions of a small number of  $\beta$  cells; then, after blood glucose levels become normal, their  $\beta$  cell clusters regenerate morphologically by creating new N1 cells to fill in the missing cells (Fig. 6). Interestingly, adult zebrafish are known to regenerate functional  $\beta$  cell clusters<sup>3,6</sup>. Ablation of  $\beta$  cells in adult zebrafish resulted in immediate hyperglycemia, followed by a recovery to almost normal levels by 7 dpa<sup>3</sup>. On the other hand, the number of  $\beta$  cells was less than half of the normal level around 7 dpa and the number of  $\beta$  cells recovered to normal levels by 17 dpa<sup>6</sup>. Taken together, these results suggest that zebrafish  $\beta$  cell clusters undergo a two-step regeneration process, first regenerating functionally and then regenerating morphologically, in adults as well as in larvae, likely throughout the entire lifespan. Therefore, we propose a definition for the phase of functional recovery during  $\beta$  cell cluster regeneration as “functional regeneration” and the phase of recovery of  $\beta$  cell numbers as “morphological regeneration.”

In this study, we found that all zebrafish  $\beta$  cells regenerate via Neurod1-expressing cells (N1 cells). The zebrafish islets already had enough N1 cells to regenerate functional  $\beta$  cell clusters immediately after  $\beta$  cell ablation (Fig. 6). Furthermore, morphological regeneration was also performed by recruiting the missing N1 cells after functional regeneration (Fig. 6). Thus, zebrafish regenerate  $\beta$  cell clusters in a very rational way, first using a minimal number of  $\beta$  cells to restore the function of the cluster, and then supplementing the missing cells to complete the regeneration.

Most previous zebrafish studies have focused on the phase of functional regeneration, which we identified in this study. They reported that  $\alpha$  cells and some endocrine progenitor cells contribute to  $\beta$  cell regeneration<sup>5,7,11</sup>. Our current results suggest that these cells already express Neurod1 or express Neurod1 within 24 hours after  $\beta$  cell ablation and that Neurod1 expression is a common characteristic of cells which give rise to the regeneration of  $\beta$  cells. On the other hand, a large number of N1 cells are present in the islets even before  $\beta$  cell ablation. Nevertheless, only a small number of  $\beta$  cells could be regenerated during functional regeneration. These results indicate that N1 cells are a heterogeneous population, some of which can give rise to regenerating  $\beta$  cells but not others. Interestingly, in our results, all regenerating  $\beta$  cells, including cells co-expressed with glucagon, were adjacent to  $\alpha$  cells (glucagon-expressing cells). Given that all  $\beta$  cells arise from N1 cells, this suggests that the regenerating  $\beta$  cells arise from N1 cells adjacent to  $\alpha$  cells (Fig. 6). In addition,  $\alpha$  cells are likely also a heterogeneous population, some of which are special  $\alpha$  cells (glucagon-expressing cells) that are able to participate in  $\beta$  cell cluster regeneration and regulate differentiation of special N1 cells to  $\beta$  cells.

We found that N1 cells for morphological regeneration are newly generated during functional regeneration. On the other hand, the question remained regarding the cells that give rise to N1 cells for morphological regeneration. Some groups have reported that centroacinar cells and ductal progenitor cells contribute to pancreatic endocrine neogenesis and  $\beta$  cell regeneration<sup>6,8,9,10,15</sup>. Interestingly, N1 cells also arise from centroacinar cells and ductal progenitor cells during endocrine neogenesis<sup>10,12,16,17</sup>. These may suggest that N1 cells for the morphological regeneration also arise from centroacinar cells

and ductal progenitor cells. On the other hand, it is unclear whether all N1 cells arise from centroacinar cells or ductal progenitor cells during endocrine neogenesis. Hence, the possibility that some N1 cells may arise from other unknown cell populations cannot currently be ruled out. To accurately understand the process of morphological regeneration, we need to clarify which cells give rise to N1 cells for morphological regeneration. If we identify these cell types, it will be a great advantage in understanding fundamental questions related to the phase of morphological regeneration, how pancreatic islets and the source cells of N1 cells sense the lack of N1 cells, how new N1 cells are generated, and how N1 cells are recruited into  $\beta$  cell clusters.

Interestingly, Neurod1 is expressed in the pancreatic islets of adult mammals<sup>18</sup>. However, it is unclear whether these N1 cells have the potential to contribute to  $\beta$  cell cluster regeneration in a similar way to zebrafish N1 cells. Further characterization of zebrafish N1 cells will reveal whether mammals also have N1 cells which can contribute to  $\beta$  cell cluster regeneration. We will then be able to propose critical methods to make completely functional  $\beta$  cell clusters in the mammalian pancreas for developing new diabetic therapies. Thus, through the results of this study, we have succeeded in making a valuable discovery that is a significant first step toward the regeneration of mammalian  $\beta$  cell clusters.

## Methods

### ***Husbandry and fish lines***

All experiments with zebrafish were approved by the Animal Care Committee of Ritsumeikan University. Zebrafish were raised and maintained under standard laboratory conditions.

We used the following transgenic lines: *Tg(insulin:loxP:mCherrySTOP:loxP:H2B-GFP;cryaa: Cerulean)*<sup>s934 19</sup>, abbreviated as *ins:Switch* or *ins:loxp-mCherry-lox-H2BGFP*, *Tg(gcga:GFP)*<sup>ia1 20</sup>, abbreviated as *gcga:GFP*, *Tg(ins:H2BGFP; ins:dsRED)*<sup>s960 2</sup>, abbreviated as *ins:H2BGFP*, and *TgBAC(neurod1:EGFP)*<sup>n11 21</sup>, abbreviated as *neurod1:EGFP*.

### ***Nitroreductase-mediated cell ablation***

To ablate pancreatic  $\beta$  cells of *ins:NTR* fish, we incubated 3 dpf larvae for 24 h in 10 mmol/L of metronidazole (Mtz; Wako Pure Chemical Industries)<sup>1 2</sup>.

### ***Fluorescence imaging***

Fluorescence images were acquired with a FV10i-DOC Laser Scanning Microscope (OLYMPUS). Cell numbers were counted manually for experiments using *ins:H2BGFP*, *gcga:GFP* with DAPI, or *ins:Switch* with DAPI. The area of mCherry in *ins:Switch* was calculated using FLOVIEW software.

### ***Glucose measurements***

Ten larvae in a group were ground up and free glucose levels were determined by using a glucose assay kit (BioVision) as described previously<sup>22 23 24</sup>.

### ***Plasmid construction and transgenesis***

To generate *-5.0neurod1:Cre* and *-5.0neurod1:CreERT2*, the *ins:Luc2* region of the *ins:Luc2;cryaa:mCherry* plasmid<sup>23</sup> was replaced with a *Cre* and *CreERT2* coding sequence downstream of 5 kb of the *neurod1* promoter<sup>21 25</sup>. The *-5.0neurod1:Cre*, *-0.8myl7:eGFP* and *-5.0neurod1:CreERT2,-0.8myl7:eGFP* plasmids was generated by replacing the *cryaa:mCherry* region of *-5.0neurod1:Cre* and *-5.0neurod1:CreERT2* with *-0.8myl7:eGFP*, respectively.

To generate each *Tg(-5.0neurod1:Cre, -0.8 myl7:EGFP)<sup>rts1</sup>* and *Tg(-5.0neurod1:CreERT2, -0.8myl7:EGFP)<sup>rts2</sup>*, the *-5kbneurod1:CreERT2:Cre-myl70.8:eGFP* and the *-5kbneurod1:CreERT2:CreERT2-myl70.8:eGFP* plasmid was co-injected with I-SceI meganuclease (New England Biolabs) into one-cell stage embryos of *RIKEN WT* as described previously<sup>26</sup>.

### ***Temporal control of CreERT2 activity***

*4-Hydroxy Tamoxifen* (4OHT; Cayman Chemical) treatment was performed at 4 to 5 dpf and 18 to 20 dpf as previously described<sup>10 15</sup>.

## **Declarations**

### **Acknowledgements**

The authors thank Dr. Didier Stainier (Max Planck Institute for Heart and Lung Research) for the *gcga:GFP*, *ins:Switch*, *ins:NTR*, *ins:H2BGFP*, and *neurod1:EGFP* lines, and Dr. David Raible (University of Washington) for plasmids of the *neurod1* promoter. *RIKEN WT* was provided by National Bio Resource Project Zebrafish. This work was supported by JSPS KAKENHI Grant Number JP20K06660, the Naito Foundation, and funds from the Ritsumeikan University to HM.

### **Author contributions**

HM conceived, designed, and performed the experiments and analyzed the data. HM and YK contributed reagents, materials, analysis, and wrote the manuscript.

## **References**

1. Pisharath, H., Rhee, J.M., Swanson, M.A., Leach, S.D. & Parsons, M.J. Targeted ablation of beta cells in the embryonic zebrafish pancreas using E. coli nitroreductase. *Mech Dev* **124**, 218–229 (2007).
2. Curado, S. *et al.* Conditional targeted cell ablation in zebrafish: a new tool for regeneration studies. *Dev Dyn* **236**, 1025–1035 (2007).

3. Moss, J.B. *et al.* Regeneration of the pancreas in adult zebrafish. *Diabetes* **58**, 1844–1851 (2009).
4. Matsuda, H. Zebrafish as a model for studying functional pancreatic  $\beta$  cells development and regeneration. *Dev Growth Differ* **60**, 393–399 (2018).
5. Ye, L., Robertson, M.A., Hesselton, D., Stainier, D.Y. & Anderson, R.M. Glucagon is essential for alpha cell transdifferentiation and beta cell neogenesis. *Development* **142**, 1407–1417 (2015).
6. Delaspre, F. *et al.* Centroacinar Cells Are Progenitors That Contribute to Endocrine Pancreas Regeneration. *Diabetes* **64**, 3499–3509 (2015).
7. Wang, H., Wei, X., Shi, W., He, J. & Luo, L. Key Developmental Regulators Suggest Multiple Origins of Pancreatic Beta Cell Regeneration. *Zebrafish* (2020).
8. Ghaye, A.P. *et al.* Progenitor potential of nkx6.1-expressing cells throughout zebrafish life and during beta cell regeneration. *BMC Biol* **13**, 70 (2015).
9. Parsons, M.J. *et al.* Notch-responsive cells initiate the secondary transition in larval zebrafish pancreas. *Mech Dev* **126**, 898–912 (2009).
10. Matsuda, H., Parsons, M.J. & Leach, S.D. Aldh1-expressing endocrine progenitor cells regulate secondary islet formation in larval zebrafish pancreas. *PLoS One* **8**, e74350 (2013).
11. Lu, J. *et al.* IGFBP1 increases  $\beta$ -cell regeneration by promoting  $\alpha$ - to  $\beta$ -cell transdifferentiation. *Embo j* **35**, 2026–2044 (2016).
12. Flasse, L.C. *et al.* Ascl1b and Neurod1, instead of Neurog3, control pancreatic endocrine cell fate in zebrafish. *BMC Biol* **11**, 78 (2013).
13. Tritschler, S., Theis, F.J., Lickert, H. & Böttcher, A. Systematic single-cell analysis provides new insights into heterogeneity and plasticity of the pancreas. *Mol Metab* **6**, 974–990 (2017).
14. Naya, F.J. *et al.* Diabetes, defective pancreatic morphogenesis, and abnormal enteroendocrine differentiation in BETA2/neuroD-deficient mice. *Genes Dev* **11**, 2323–2334 (1997).
15. Wang, Y., Rovira, M., Yusuff, S. & Parsons, M.J. Genetic inducible fate mapping in larval zebrafish reveals origins of adult insulin-producing  $\beta$ -cells. *Development* **138**, 609–617 (2011).
16. Kimmel, R.A., Onder, L., Wilfinger, A., Ellertsdottir, E. & Meyer, D. Requirement for Pdx1 in specification of latent endocrine progenitors in zebrafish. *BMC Biol* **9**, 75 (2011).
17. Ninov, N., Borius, M. & Stainier, D.Y. Different levels of Notch signaling regulate quiescence, renewal and differentiation in pancreatic endocrine progenitors. *Development* **139**, 1557–1567 (2012).
18. Gu, C. *et al.* Pancreatic beta cells require NeuroD to achieve and maintain functional maturity. *Cell Metab* **11**, 298–310 (2010).
19. Hesselton, D., Anderson, R.M. & Stainier, D.Y. Suppression of Ptf1a activity induces acinar-to-endocrine conversion. *Curr Biol* **21**, 712–717 (2011).
20. Zecchin, E. *et al.* Distinct delta and jagged genes control sequential segregation of pancreatic cell types from precursor pools in zebrafish. *Dev Biol* **301**, 192–204 (2007).
21. Obholzer, N. *et al.* Vesicular glutamate transporter 3 is required for synaptic transmission in zebrafish hair cells. *J Neurosci* **28**, 2110–2118 (2008).

22. Gut, P. *et al.* Whole-organism screening for gluconeogenesis identifies activators of fasting metabolism. *Nat Chem Biol* **9**, 97–104 (2013).
23. Matsuda, H., Mullapudi, S.T., Zhang, Y., Hesselton, D. & Stainier, D.Y.R. Thyroid Hormone Coordinates Pancreatic Islet Maturation During the Zebrafish Larval-to-Juvenile Transition to Maintain Glucose Homeostasis. *Diabetes* **66**, 2623–2635 (2017).
24. Matsuda, H. *et al.* Whole-Organism Chemical Screening Identifies Modulators of Pancreatic  $\beta$ -Cell Function. *Diabetes* **67**, 2268–2279 (2018).
25. McGraw, H.F., Snelson, C.D., Prendergast, A., Suli, A. & Raible, D.W. Postembryonic neuronal addition in zebrafish dorsal root ganglia is regulated by Notch signaling. *Neural Dev* **7**, 23 (2012).
26. Thermes, V. *et al.* I-SceI meganuclease mediates highly efficient transgenesis in fish. *Mech Dev* **118**, 91–98 (2002).

## Figures

Figure 1

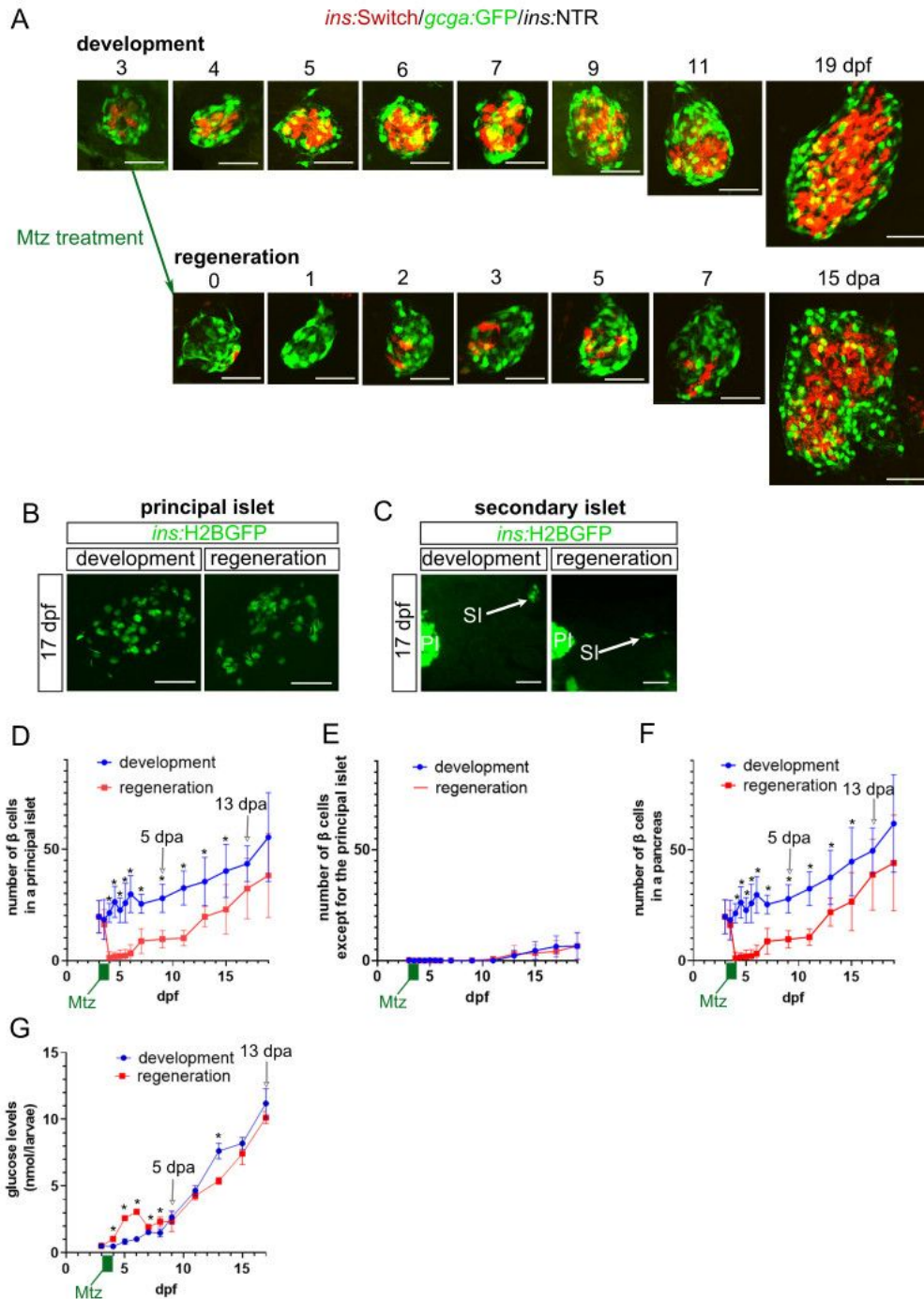


Figure 1

**Zebrafish can regenerate pancreatic  $\beta$  cell functionally and morphologically.** (A) Morphological changes of the pancreatic islet (*gcga:GFP*,  $\alpha$  cell; *ins:Switch*,  $\beta$  cell) during development and  $\beta$  cell regeneration. (B) The phenotype of the principal islet in animals treated with or without Mtz at 17 dpf (13 dpa). (C) The phenotype of secondary islets (SI) in animals treated with or without Mtz at 17 dpf (13 dpa). (D) Changes in the number of  $\beta$  cells in the principal islet of animals treated with or without Mtz (mean  $\pm$  STD; n = 8–

11). (E) Changes in the number of  $\beta$  cells in the secondary islets of animals treated with or without Mtz (mean  $\pm$  STD; n = 8–11). (F) Changes in the total number of  $\beta$  cells in the pancreas of animals treated with or without Mtz (mean  $\pm$  STD; n = 8–11). Note that the difference in the number of  $\beta$  cells between development and  $\beta$  cell regeneration were no longer significant at 17 dpf (13 dpa). (G) Change of glucose levels in animals treated with or without Mtz (mean  $\pm$  STD; n = 3). Note that the difference in whole glucose levels between development and  $\beta$  cell regeneration were no longer significant at 9 dpf (5 dpa). \*P < 0.05 compared with control development samples of the same age by Student's t-test. Scale bars, 40  $\mu$ m. dpf, days post-fertilization; dpa, days post- $\beta$  ablation; PI, principal islet.

Figure 2

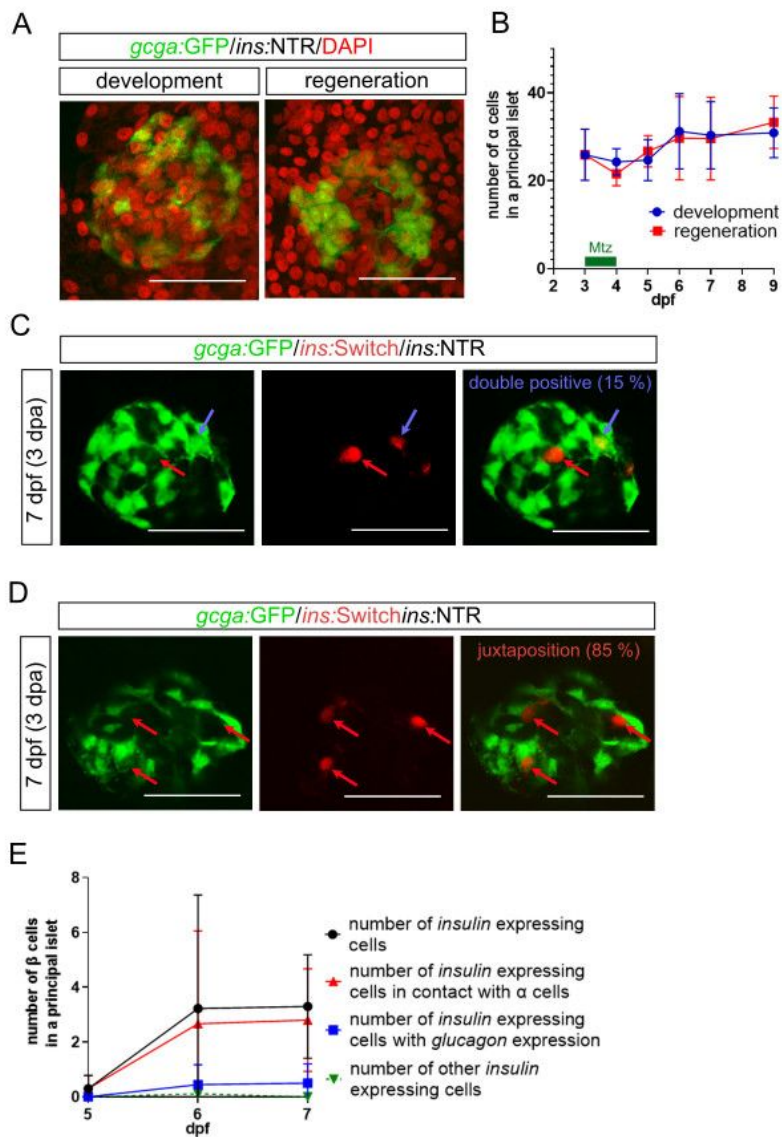


Figure 2

**Regenerating pancreatic  $\beta$  cells in direct contact with  $\alpha$  cells.** (A) Morphology of pancreatic  $\alpha$  cells (*gcga:GFP*-expressing cells) in animals treated with or without Mtz at 5 dpf (1 dpa). (B) Changes in number of  $\alpha$  cells in the principal islet in animals treated with or without Mtz (mean  $\pm$  STD; n = 9–10). (C–D) Relationship of the localization between  $\alpha$  cells and regenerating  $\beta$  cells (*ins:Switch*-expressing cells) at 3 dpa. (E) Quantification of the relationship of localization between  $\alpha$  cells and regenerating  $\beta$  cells

(mean  $\pm$  STD; n = 9–10). Note that 15% of regenerating  $\beta$  cells were *gcga*:GFP-expressing cells at 3 dpa (C and E) and that 85% of regenerating  $\beta$  cells were juxtaposed to *gcga*:GFP-expressing cells at 3 dpa (C and E). Scale bars, 40  $\mu$ m.

Figure 3

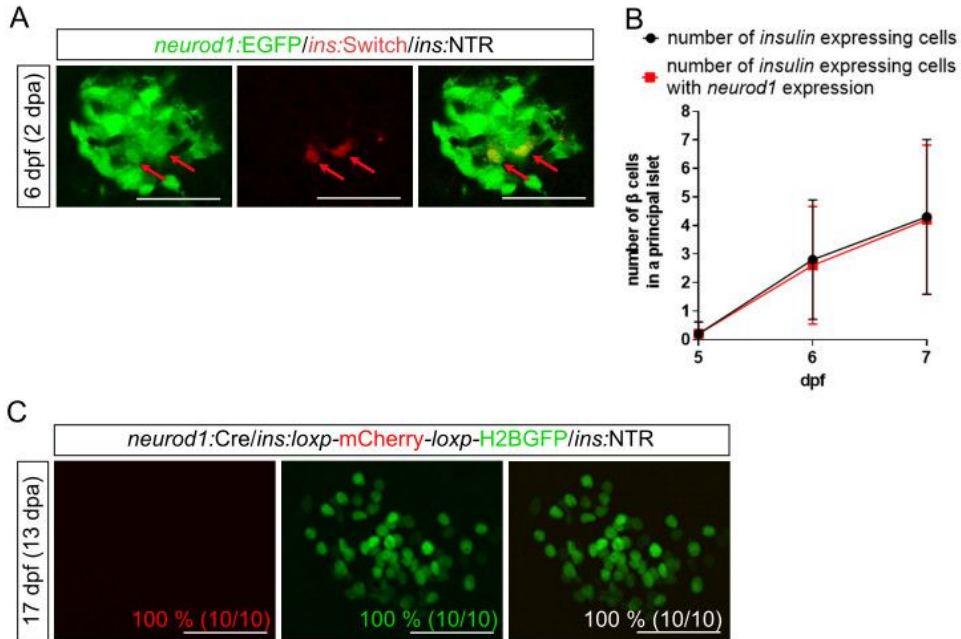


Figure 3

**All regenerating  $\beta$  cells arose from Neurod1-expressing cells.** (A) Relationship of the localization between *neurod1*:EGFP-expressing cells and regenerating  $\beta$  cells (*ins*:Switch-expressing cells) at 2 dpa. (B) Quantification of the relationship of localization between *neurod1*:EGFP-expressing cells and regenerating  $\beta$  cells between 1 and 3 dpa (5 and 7 dpf) (mean  $\pm$  STD; n = 10). Note that most regenerating  $\beta$  cells are *neurod1*:EGFP-expressing cells (A and B). (C) Phenotypes of *neurod1*:Cre/*ins*:*loxp*-mCherry-*loxp*-H2BGFP/*ins*:NTR at 13 dpa (17 dpf), which distinguished  $\beta$  cells that arose from Neurod1-expressing cells (green cells) and other cells (red cells). Note that all regenerating  $\beta$  cells arose from Neurod1-expressing cells. Scale bars, 40  $\mu$ m.

Figure 4

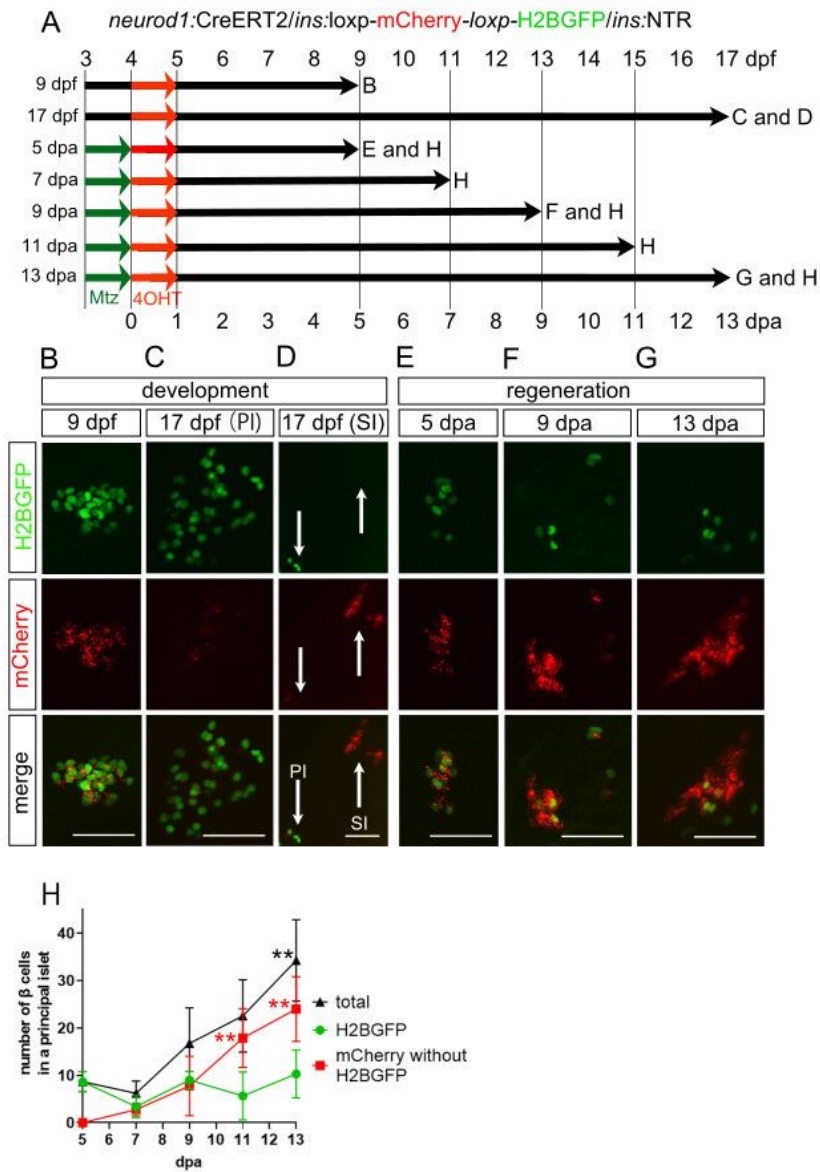
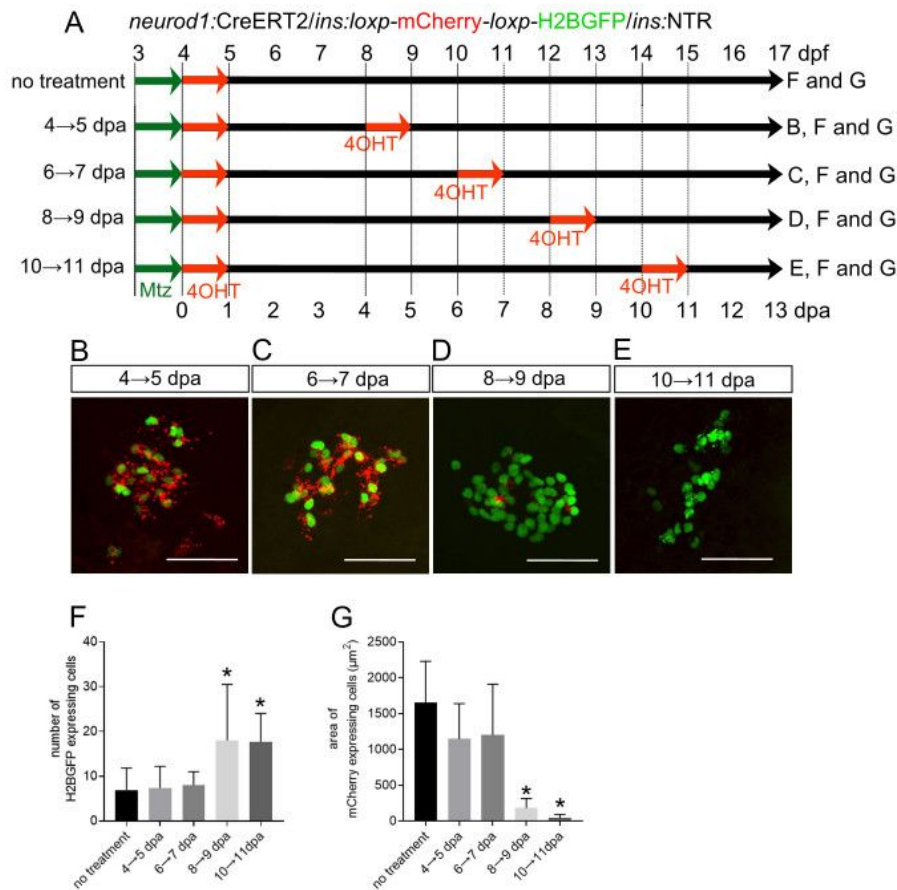


Figure 4

**Different cell lineages of Neurod1-expressing cells contribute to  $\beta$  cell regeneration, but not pancreatic development.** (A-G) *neurod1:CreERT2/ins:loxp-mCherry-loxp-H2BGFP/ins:NTR* lines were treated with 4-Hydroxy Tamoxifen (4OHT) between 4 and 5 dpf (red arrows in A) with or without Mtz treatment between 3 and 4 dpf (green arrows in A), and then sacrificed for analysis at 9 (B and E), 13 (F), or 17 dpf (C, D, and G). Note that all developing  $\beta$  cells in the principal islet (PI), but not secondary islets (SI), arose from

Neurod1-expressing cells from 4 to 5 dpf. (H) Quantification of changes in the number of regenerating  $\beta$  cells with H2BGFP and/or mCherry expression (mean  $\pm$  STD; n = 5–10). Note that the number of H2BGFP-expressing cells did not change, but the number of mCherry-expressing cells without H2BGFP expression was significantly increased during  $\beta$  cell regeneration after 11 dpa. \*\*P < 0.01 compared with samples at 5 dpa by Tukey's honestly significant difference test after ANOVA. Scale bars, 40  $\mu$ m. PI, principal islet cells; SI, secondary islet cells.

Figure 5



## Figure 5

**Most new Neurod1-expressing cells rapidly generate after 7 dpa.** (A-F) *neurod1:CreERT2/ins:loxp-mCherry-loxp-H2BGFP/ins:NTR* lines were treated with 4OHT (red arrows in A) between 4 to 5 (B), 6 to 7 (C), 8 to 9 (D), or 10 to 11 dpa (E) after treatment with Mtz from 3 to 4 dpf (green arrows in A) and 4OHT from 4 to 5 dpf, and then sacrificed for analysis at 17 dpf. (F) Quantification of changes in the number of regenerating  $\beta$  cells with H2BGFP expression (mean  $\pm$  STD; n = 9). (G) Quantification of the area of regenerating  $\beta$  cells with mCherry expression (mean  $\pm$  STD; n = 9). Note that the number of H2BGFP-expressing cells was elevated after 7 dpf and that the area of mCherry-expressing cells was reduced after 7 dpf. \*P < 0.05 compared with samples at 5 dpa by Tukey's honestly significant difference test after ANOVA. Scale bars, 40  $\mu$ m.

Figure 6

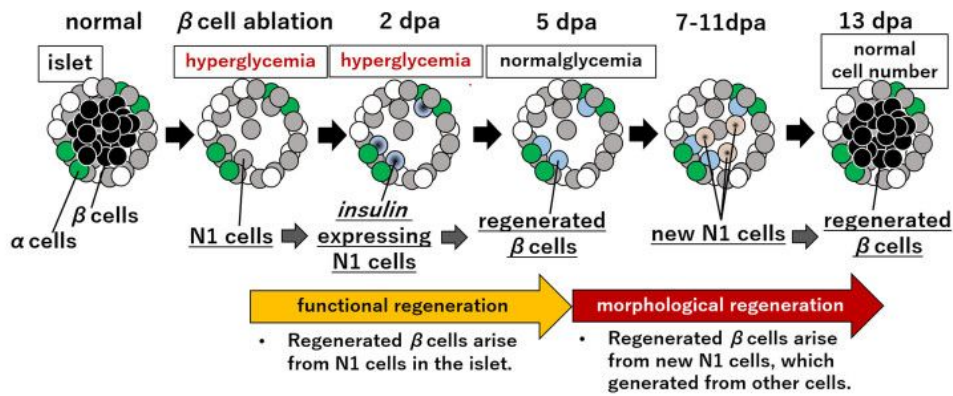


Figure 6

**A model for pancreatic  $\beta$  cell regeneration in zebrafish.** Zebrafish islets regenerate the functionality and morphology of  $\beta$  cell clusters in a stepwise manner. First, Neurod1-expressing cells (N1 cells) in the islets are utilized to recover cluster function with fewer  $\beta$  cells than normal, and then missing N1 cells are newly generated to regenerate the morphology after returning to normoglycemia.